UC Davis

UC Davis Previously Published Works

Title

High Pressure Aqueous Geochemical NMR

Permalink

https://escholarship.org/uc/item/4867q0dk

Journal

EMAGRES, 8(2)

ISSN

2055-6101

Authors

Pilgrim, Corey D
Casey, William H
Walton, Jeffrey H

Publication Date

2019

DOI

10.1002/9780470034590.emrstm1612

Peer reviewed

eScholarship.org Powered by the California Digital Library
University of California

High Pressure Aqueous Geochemical NMR

Corey D. Pilgrim[1], William H. Casey[1] & Jeffrey H. Walton[2]

[1] *Department of Chemistry, University of California-Davis, Davis, CA, USA*
[2] *NMR Facility, University of California-Davis, Davis, CA, USA*

High-pressure NMR has been in existence or 65 years and has evolved to be an essential tool for many disciplines. High-pressure NMR is useful both for determining standard thermodynamic properties and for assigning mechanisms of aqueous ligand-exchange reactions since solvation changes are sensitive to pressure. There have been many different apparatuses to provide and maintain pressure to the chemical systems of interest. Of these different devices, our group has primarily used the clamp-cell probe design, which allows for study of aqueous solute species that are important to geochemistry and at conditions seen in the crust and upper mantle of the Earth. ^{11}B and ^{29}Si studies are reviewed herein, and directions of future progress in the field are provided.

Keywords: high-pressure, geochemistry, reaction kinetics, ^{29}Si aqueous silicate complexes, ^{11}B boric acid–catecholate complexes, high-pressure NMR probe design, activation volume

How to cite this article:
eMagRes, 2019, Vol 8: 127–136. DOI 10.1002/9780470034590.emrstm1612

Introduction

Interest in high-pressure nuclear magnetic resonance (NMR) has been consistent since the technique was first introduced by Benedek and Purcell in 1954.[1] While initially used to examine the pressure and volume dependencies of the Knight shift in different metals[2,3] as well as the relaxometry and diffusion within many materials,[4,5] the technique has evolved to provide a wide range of useful information about the structure and dynamics of chemical systems and has shown use in solid-state physics,[6,7] polymer chemistry,[8] geochemistry,[9] and even biochemistry, where the motions of proteins are examined.[10]

Interpretation of high-pressure experiments relies on the basic thermodynamics, including Gibbs free energy (G), defined as:

$$G = U + PV - TS \tag{1}$$

where U is the internal energy of the system, P is the pressure, V is the volume, T is the temperature, and S is the entropy. Taking the derivative of this equation and substituting in the first law of thermodynamics ($\mathrm{d}U = T\mathrm{d}S - P\mathrm{d}V$) yields:

$$\mathrm{d}G = V\mathrm{d}P - S\mathrm{d}T \tag{2}$$

Rearranging the differentials for pressure while holding the system under isothermal conditions yields the final equation relating pressure to reaction volume:

$$\left(\frac{\mathrm{d}G}{\mathrm{d}P}\right)_T = V \tag{3}$$

From equation (3), the state variable of volume, or change in volume for a reaction, becomes key to these high-pressure measurements. Equation (3) indicates that the partial molar volume of any species under observation dominates the pressure variation of a reaction, especially so in aqueous environments where the large partial molar volume of water (18 cm^3 mol^{-1} at 25 °C) plays a large role in determining the conformation of molecules. Stated differently, high-pressure NMR can sensitively follow changes in reactions that involve altered solvation states, such as reactions that change metal coordination numbers.

Transition-state theory links equilibrium and disequilibrium thermodynamics and establishes that there is an unstable activated state in a chemical reaction that is intermediate between reactants and products.[11,12] Most of the same algebra describing chemical equilibrium applies to a metastable equilibrium between reactants and this activated state. Some amount of energy is needed to initiate this change from reactant to the transition state. Here, we denote this activation energy as $\Delta G^{\ddagger}$. This activation energy is treated similarly to the standard thermodynamic Gibbs free energy, such that the analog to equation (3) for disequilibrium becomes:

$$\left(\frac{\mathrm{d}G^{\ddagger}}{\mathrm{d}P}\right)_T = V^{\ddagger} \tag{4}$$

The volume defined in equations (3) and (4) are known as a reaction volume for conventional equilibrium reaction [equation (3)], or an activation volume (denoted $\Delta V^{\ddagger}$) for a disequilibrium process [equation (4)]. The magnitude and sign of $\Delta V^{\ddagger}$ provides information on the size of the transition state relative to the reactants, and thus information about the pathway. Reactions are described as having associative or dissociative characters depending upon the volume change, changes in coordination number, and the involvement of the incoming ligand in the transition state. In practice, a

© 2019 John Wiley & Sons, Ltd.

continuum exists between the purely associative or dissociative reaction pathways. $\Delta V^{\ddagger}$ has been rigorously studied for many systems and has been recently reviewed.[13–15] The measurement of $\Delta V^{\ddagger}$ is accomplished by measuring the rates of reaction (k) as a function of pressure using the Eyring–Polanyi equation:

$$\left(\frac{\mathrm{d}(\ln k)}{\mathrm{d}P}\right)_T = -\frac{\Delta V^{\ddagger}}{RT} \tag{5}$$

where R is the gas constant and T is the temperature. The method for using NMR to measure the rates of these reactions is extensively covered in the literature,[16–19] and when coupled with high-pressure apparatus, information about the rates and mechanisms of elementary reaction steps can be obtained.[20]

Review of High-pressure Approaches in NMR

The original apparatus used for high-pressure NMR consisted of a beryllium-copper (BeCu) vessel setup similar to that detailed by Bridgman,[21] where the pressure was generated via an umbilical pipe that contained the pressure-transmission fluid. The field has expanded within the last 65 years as numerous designs for high-pressure devices have been published, each with their own unique advantages. This section will review the different probe designs, but first, something must be said for how the pressure is calibrated within these devices.

Pressure to these types of probes is generally applied using either a pump/intensifier to drive a pressure-transfer medium (liquid or gas) in-line to the probe, or through a press-force that is maintained through a locking assembly on the probe itself. Ideally, the pressure is hydrostatic in nature, such that the pressure is uniform around the sample, and is usually achieved by immersing the sample in liquid. Hydrostatic conditions are essential to prevent anisotropy introduced by the pressurization as well as minimize hysteresis in the sample. Ordinarily, pressure is measured using a Bourdon-type pressure gauge, but these can be unreliable when determining pressure inside a probe. One of the primary ways to calibrate the pressure within these probes is to measure the resistance of a wire within the pressurized environment, as the resistance of metal will change with pressure. It was very early shown that manganin wire (an alloy of copper, manganese, and nickel) produces a linear response to pressure, increasing in resistance with increasing pressure.[22–24] This approach was the standard for pressure calibration for many years within the field and is still used today in some applications. While robust, the manganin-wire gauge can be somewhat difficult to manipulate, especially at the very small gauges of wire used, and the size requirement for the coil of wire is too large for the modern diamond-anvil cell (DAC) probes. Also, manganin wire is magnetic, so it is not ideal for modern magnetic resonance applications, especially in high-field magnets. To avoid these problems, an alternative calibration method was devised. The R_1 fluorescence peak of a ruby (specifically from the Cr^{3+} present in the structure) was shown to vary linearly with pressure.[25] This technique has proven to be extremely useful with the rise of cheap spectrometers and fiber-optic cables. The small size of the ruby needed, and the ability to optically couple the ruby fluorescence via fiber-optic cable, has made this the pressure-measurement method of choice for extremely high pressures.[26,27]

Two important remarks must be made about high-pressure designs. First, many physical measurements require a 'feedthrough' to introduce wire or fiber-optics into the chamber. This feedthrough creates a weak point in the design that are prone to catastrophic pressure release. Thus, the most robust designs have the fewest feedthroughs. Secondly, both gases and liquids have been used as pressure-transfer media. However, due to the compressibility of gases, a great deal of energy is stored in the system. Upon uncontrolled release, a great deal of damage and harm to the surroundings can occur. As such, it is not advised to use gases in this manner and liquid pressure-transfer media have become the modern standard in high-pressure research because they are safer.

BeCu Pressure Bomb

Benedek and Purcell used pressure bombs in their initial experiments and the design has changed little over the years.[1] These devices consist of a Bridgman-type press that forces pressure-transmitting fluid into the coupled probe via an in-line umbilical tube. This fluid is fed into a BeCu body; the overall vessel is shown in cross-section in Figure 1(a). To segregate the pressure-transmission fluid from the liquid sample, a sample holder is placed within the pressure bomb and the pressure-transmission fluid contacts the top of the holder and compresses the unit down using the built-in metal sylphon as shown in cross-section in Figure 1(b). The NMR coil is immersed within this sample holder, which thus achieves a large filling factor. However, this type of probe must be placed within the magnetic field, which yields challenges as a large mass of metal (though nonmagnetic) is placed within the center of the magnetic field of an NMR magnet. These probes can reach up to 1.0 GPa in pressure without difficulty.

Jonas-type Pressure Vessel

Other than the switch to titanium casings in some probe designs,[7,8] the standard pressure vessel has not seen many external revisions (we note here that ethanol should not be used as a pressure transmission media with titanium pressure vessels due to ethanol becoming chemically reactive with titanium under pressure). However, the sample compartment within the vessel has undergone many revisions to reduce the sample volume.[5,28–31] The sample compartment evolved away from the metal sylphon used in the initial Benedek and Purcell design towards use of a glass syringe with a plunger, as can be seen in the initial work by Jonas *et al.*[32] Their design was used and refined throughout the years (Figure 2)[33–35] and has seen use elsewhere in the literature.[36,37] The latest version of their design couples the glass sample holder with a single-turn saddle coil (Figure 2, inset) to provide better sensitivity to the NMR measurements in high field superconducting magnets.[38] This design shares the disadvantages of the original pressure bombs as the probe body is large, metallic, and constantly connected to a pressure source, while the change in sample compartments limits the pressure to less than around 0.5 GPa.

© 2019 John Wiley & Sons, Ltd.

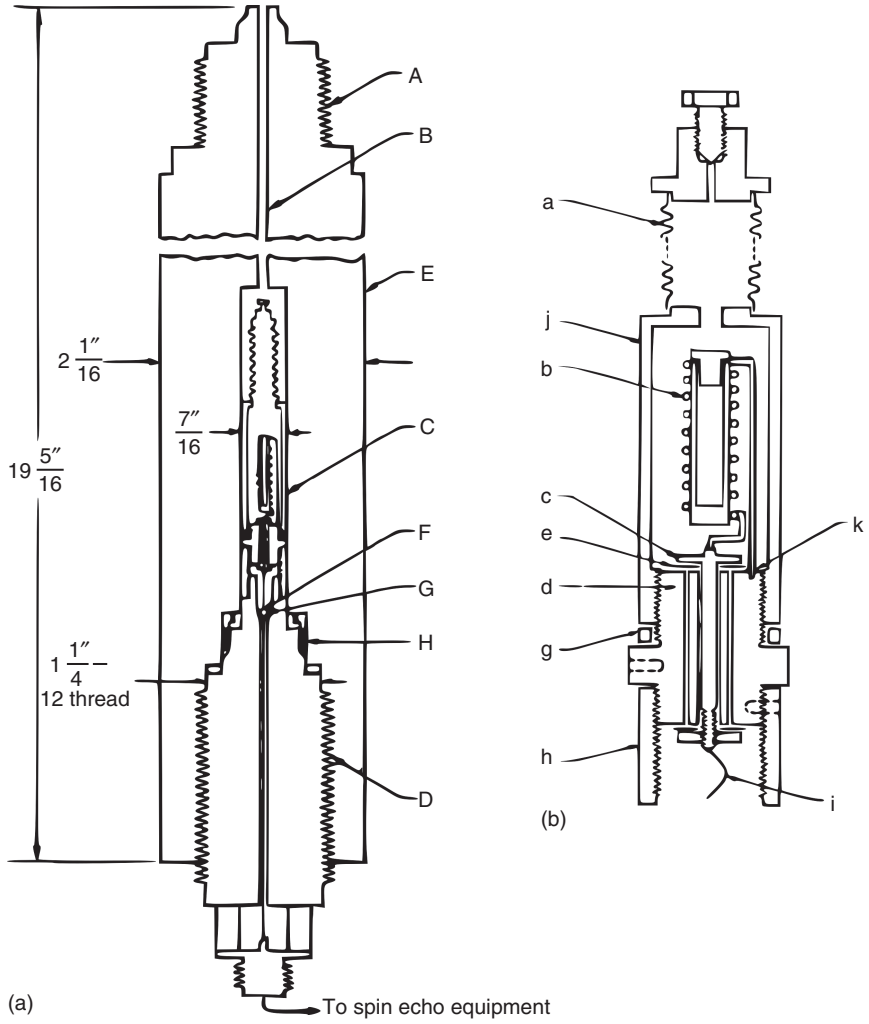

Figure 1. (a) The cross-section of a BeCu pressure bomb. (b) The cross-section of the sample holder allows for segregation of the sample from the pressure-transmission fluid.[1] (Reprinted from Benedek, G. B.; Purcell, E. M. Nuclear Magnetic Resonance in Liquids under High Pressure. *J. Chem. Phys.* **1954**, *22* (12), 2003–2012, with the permission of AIP Publishing)

Anvil-type Probes

The main limitation to the Jonas pressure vessel design is that, due to the geometry of the probe, pressures beyond 0.5 GPa cannot be easily achieved. To circumvent these limits, the high-pressure cell was redesigned to use the anvil design, initially using Al_2O_3–TiO_2 as the anvil,[39] though conversion to a DAC was bound to follow.[40] The benefits of these anvil probes are numerous, as with the reduction of sample volume, applied pressure becomes much greater (initially upwards of 7.0 GPa[41] though improvements in this ceiling will be discussed later) and the need for umbilical lines to constantly provide the pressure were eventually eliminated. The initial drawbacks of the design were low sensitivity, a very small sample, and the RF coils that were placed outside the gaskets of the anvil, which effectively shielded the sample and provided a lower filling-factor and sensitivity. Cross-sections of these types of probes are presented in Figure 3. One added benefit of the DAC is the direct measurement of pressure inside the cell through ruby fluorescence, as ruby chips can be incorporated into the sample volume and the fluorescence can be induced and measured through the translucent diamonds.[42]

In recent years, research has focused on the improvement of resonators within DAC designs to combat the sensitivity issues. While there were efforts to redesign the external resonator,[41,43,44] there has been success in inserting the RF coil within the DAC.[45,46] This microcoil design allows for an increased filling factor and reduces the influence of the gasket on the magnetic field produced by the coil. This design has since been modified to include Lenz lenses within the DAC structure and to eliminate the coil from within the sample compartment, which also reduces the need for a feedthrough for wire, which is a main source of failure. With these improvements, the pressure ceiling of these NMR measurements has been increased to above 70.0 GPa.[47] With this type of design, the sample volumes are kept extremely small (near 100 pL in volume) which reduces the total number of spins available for measurement within the sample coil.

© 2019 John Wiley & Sons, Ltd.

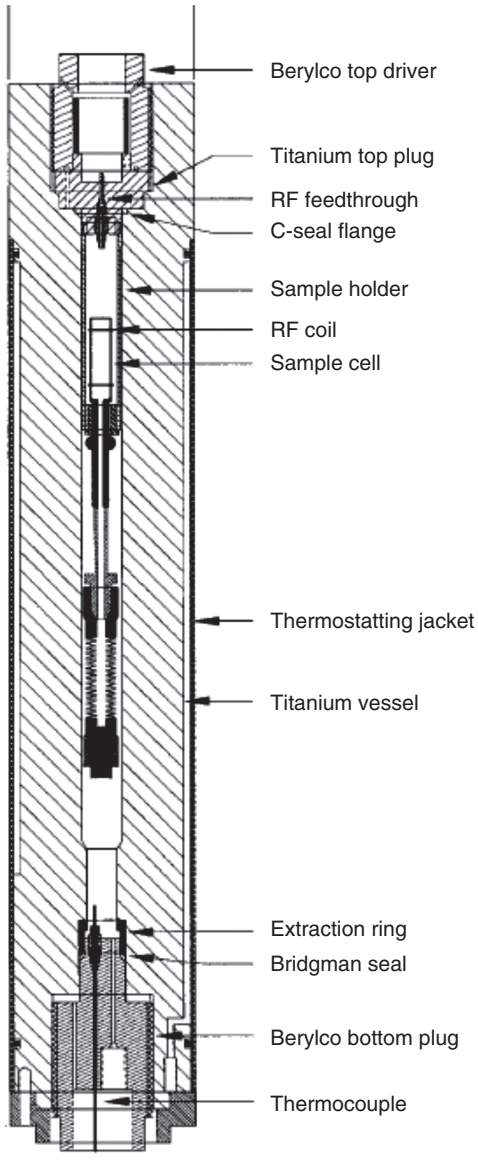

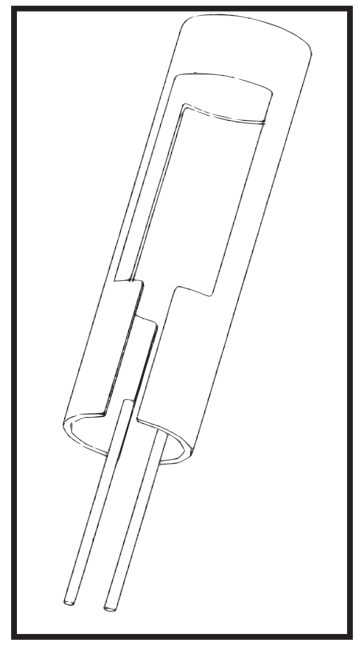

Figure 2. Cross-section of a Jonas-type pressure vessel. This design includes a thermostatting jacket to provide a steady temperature environment to the sample. In the design shown here, a bellows is used to allow for the volume change in the sample compartment, though a plunger is just as feasible. The inset shows the design for the single-turn saddle coil.[35,38] (Adapted from Ballard 1996 and Ballard 1998)

Clamp-cell Probes

The clamp-cell design for high-pressure measurements has been around for almost 40 years.[48–50] It has only been recently adapted for use in high-pressure NMR experiments.[9,51,52] This probe type is somewhat of a compromise between the pressure-bomb and DAC designs and allows for study of solute chemistry. This design currently allows for pressure generation above 2.0 GPa. The volume used is orders of magnitude larger than in the DAC (typically these probes use between 10 and 500 μL of solution). This probe consists of a moderate mass of BeCu (a diamagnetic metal), coupled with internal tungsten carbide (WC, a paramagnetic metal) components, so there are still issues with shimming the system for magnetic homogeneity, though steps to minimize the amount of metal and coupling with a high-powered shim supply have been taken to help mitigate this (see sections titled 'Current Geochemical Research' and '^{29}Si NMR study'). However, like the DAC, this system does not require an umbilical tube to provide constant pressure – the pressure is generated via hydraulic press, but the internal piston is held in place via a lock nut on the end of the probe (Figure 4). The NMR circuit consists of a microcoil similar to that in the more recent DAC designs. The original design was for wide-bore magnet systems but has since been reduced in size to allow for use in modern narrow-bore magnets.

High-pressure Glass Tubes

The final design that will be discussed is one in which the high-pressure apparatus is not a probe but is designed to fit within commercially available probes. This approach was initially

© 2019 John Wiley & Sons, Ltd.

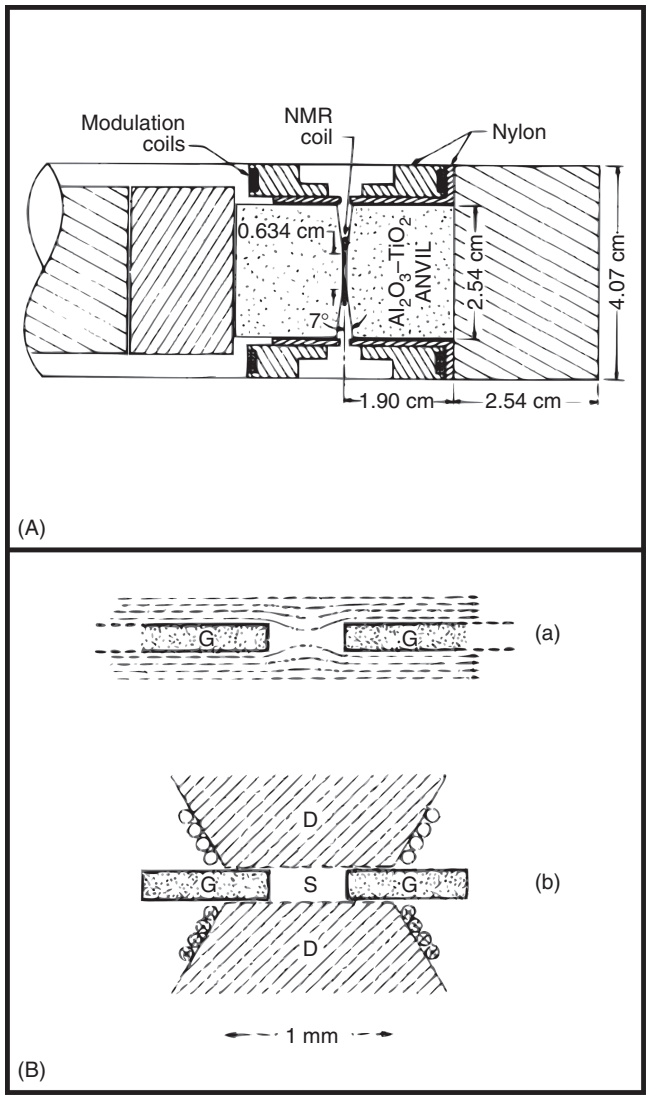

Figure 3. (A) Cross-section of the initial Bridgman-type anvil design, showcasing the smaller sample volume. Notice how the NMR coil is placed outside the gasket/sample compartment.[39] (Reprinted from Vaughan, R. W.; Lai, C. F.; Elleman, D. D. An Apparatus for Magnetic Measurements at High Pressure. *Rev. Sci. Instrum.* **1971**, *42* (5), 626–629, with the permission of AIP Publishing.) (B) (a) Influence of the gasket within a DAC on the induced magnetic field. (b) Cross-section of the DAC design, specifically the sample volume. In this image, *D* denotes diamond, *G* denotes gasket, and *S* denotes sample. In this design, the NMR coil is placed outside the gasket.[40] (Reprinted from Lee, S. H.; Luszczynski, K.; Norberg, R. E.; Conradi, M. S. NMR in a Diamond Anvil Cell. *Rev. Sci. Instrum.* **1987**, *58* (3), 415–417, with the permission of AIP Publishing)

conceived by Yamada *et al.* to provide high-resolution NMR spectra through the use of specialized glass tubes that were connected via umbilical capillary to a hand-pump.[53] This design was improved upon and commercialized by Daedalus Innovations, LLC.[54] A BeCu assembly is attached to a sapphire tube which contains the sample and is placed within the commercial NMR probe. Pressure is applied using a capillary umbilical tube that is connected to a computer-activated syringe pump. The pressure-transfer fluid is typically ethanol, which supplies pressure to the sample via a set of plungers so that there is no mixing with the aqueous samples. This apparatus has been used in conjunction with the technique of encapsulating proteins in reverse micelles to provide remarkable structural information.[10,55–59] While this approach has a relatively small achievable pressure (~0.11 GPa), it is a reasonable method for studying proteins where larger sample volumes are necessary and where the reaction volumes for conformational changes, such as protein unfolding, are large.

Current Geochemical Research

High-pressure NMR is well suited for examining the geochemistry of the Earth's crust and upper mantle where liquid water exists. At pressures of a few GPa, scientists can follow the behavior of chemical species affected by pressures 1–50 km within the Earth, which spans the deepest thickness of crust and to the upper mantle. Kozlovsky has observed brines at these depths,[60] and water still acts as the main transport for electrolytes, but

© 2019 John Wiley & Sons, Ltd.

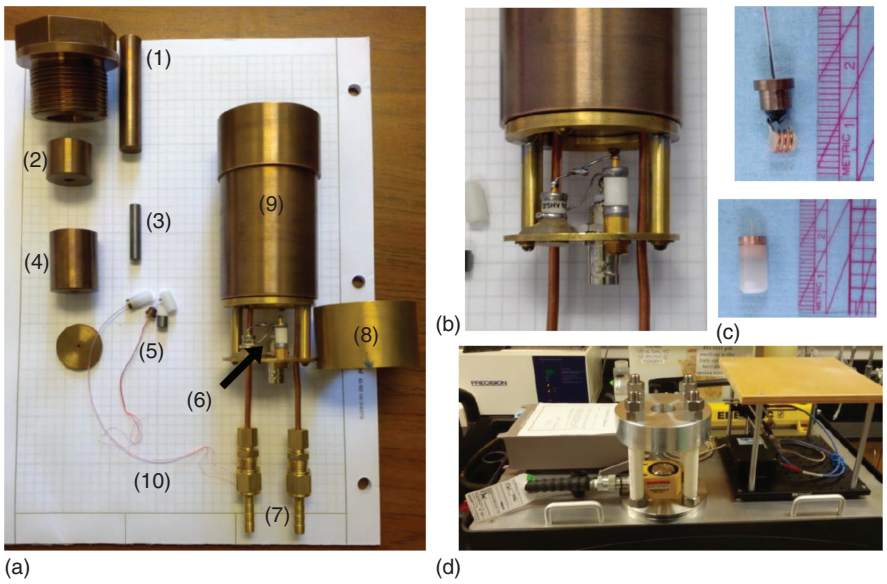

Figure 4. The clamp-cell probe design is shown. A completely disassembled probe, with the body (9), locknut (1), inner cylinders (2, 4) consisting of BeCu, while the internal piston (3) is WC are all shown in (a). The electronics are housed on the top of the probe and shielded by the brass sheath (8) and can be seen clearly in (b). The feedthrough assembly (5) is also seen clearly in (c), where the microcoil geometry is evident. Finally, the press and spectrometer set-up used to provide and measure the pressure within the probe is shown in (d).[9] (Reproduced with permission from Ref. 9. © John Wiley and Sons, 2014)

the chemistry of these aqueous species is largely unprobed by NMR. There are models that hypothesize what reactions occur, and one well-accepted model over the last 30 years has been the Helgeson–Kirkham–Flowers (HKF) model.[61–64] This model extrapolates partial molal properties, activity coefficients, solvent dielectrics, and other parameters for aqueous electrolytes from standard states up to 600 °C and 0.5 GPa in pressure. The model was limited by data about the static permittivity of water until recently when it was extended to 1200 °C and 6 GPa via computer simulations.[65,66] NMR is well suited to measure the thermodynamics and kinetics of solutes in aqueous solutions and the design of the clamped-cell was optimized with this goal in mind.

^{11}B NMR Study

In the first use of the clamp-cell design for NMR, solutions of boric acid and boric acid–catecholate complexes were examined up to 1.2 GPa in pressure using the ^{11}B nucleus.[9] Boric acid and its derivatives provide an interesting case study: from the Deep Earth HKF model, it was speculated that the dissociation constant of boric acid would increase eight orders of magnitude as pressure increases from ambient to 2.0 GPa.[66] Experimentally (and visualized in Figure 5a), the effects of pressure are quite noticeable on the spectra for the sodium-borate system. At ambient conditions, there were two resonances seen – one corresponding to a polyborate species (14.3 ppm) and one to the single tetraborate species (8.9 ppm). As pressure was increased, the polyborate species disappeared and a single peak belonging to the single borate species was observed. This follows the trend that at increased pressure, the system wants to reduce the overall volume, and the easiest way is to pack more water into the coordination sphere of metals. Additional waters are packed into the coordination sphere of boron as polyborate species hydrolyze into monomeric units.

The second part of this project was to look at the dynamics of exchange of boric acid–catecholate species under pressure. In Figure 5, the NMR spectra are visualized from selected solution compositions, specifically a solution with lower pH and higher catechol content (Figure 5b) and a solution with higher pH and higher boric acid content (Figure 5c). Coalescence with pressure was observed in 5B while not in 5C, which lead to the conclusion that tetrahedral borate species are not as capable of complexing 1,2-diol ligands as is the trigonal boric acid. From these (and other) measurements, activation volumes of the boric acid–catecholate complexes were calculated to be approximately $-13.9 \pm 2.2\ \mathrm{cm^3\ mol^{-1}}$, which suggested that the complexation is accompanied by electrostriction, which arises from changes in the solvation energy of the charged complex because of changes in the dielectric permittivity with pressure.

^{29}Si NMR Study

One of the latest projects to use the clamp-cell NMR design was the examination of aqueous silicate complexes at elevated pressures using ^{29}Si NMR.[52] One of the challenges with these types of probes is the resistance to shimming that is expected from the introduction of two large quantities of metals, with very different magnetic susceptibilities, into the bore of the superconducting magnet. To offset this, the original probe design was reduced to fit in modern narrow-bore instruments while maintain the inner geometry and was coupled with a custom-made high-power shim stack from Resonance Resources, Inc. (Billerica, Massachusetts, USA). This high-current shim stack allowed for shimming on a D_2O resonance using a tuned ^{2}H circuit such

© 2019 John Wiley & Sons, Ltd.

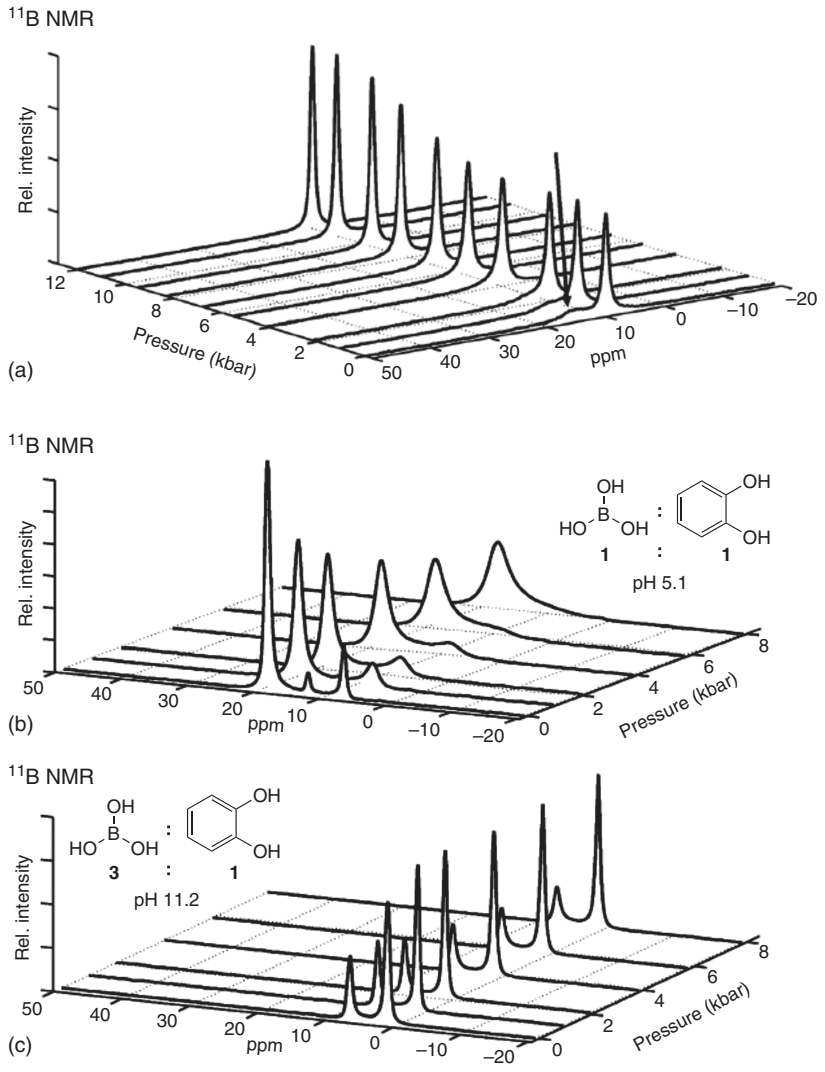

Figure 5. (a) ^{11}B spectra from the borate solution. As pressure is increased, the polyborate species (14.3 ppm) disappears. (b) ^{11}B spectra from the boric acid–catechol system, where the ratio is 1 : 1. As pressure is increased, coalescence is seen between the three peaks, indicating exchange is occurring. (c) ^{11}B spectra from the boric acid–catecholate system again, though with a ratio of 3 : 1 in favor of boric acid and a much higher initial pH. Surprisingly, coalescence is not seen, which suggests a lowered reactivity of the borate species with catechol.[9] (Reproduced with permission from Ref. 9. © John Wiley and Sons, 2014)

that linewidths on the order of 30 Hz were achievable at ambient conditions.

Using this apparatus, three different solutions of silicates were examined up to 1.8 GPa in pressure: silicate oligomers, a silicate–sugar complex, and a silicate–catecholate complex. In each case, different bonding environments of the silicates were evident, with 4-, 5-, or 6-coordinate silicon apparent in the solutions throughout the study. An example of the spectra for the oligomeric silicate species is shown in Figure 6. In two of the three cases (the oligomers and the silicate–sugar complex), changes in the bonding environments were clearly evident with changes in pressure. The changes were interpreted to indicate that more efficient packing of water at pressure led to the loss of extended coordination in the silicate species because complexation required transfer of water to, or from, the bulk. In the third case, the silicate–catecholate complex, no change in the bonding environment was seen, other than a broadening of the resonance at high pressure. This observation was interpreted to indicate that the solution reached a freezing point before the very strong catecholate complex would dissociate into the silicate monomer, which was surprising in light of the other measurements. No evidence of dissociation was found.

Future Directions

The examples above demonstrate that the properties of aqueous solutions can be studied using high-pressure NMR at pressures corresponding to pressures deep inside the Earth. The changes with pressure are not subtle, nor well understood. The dielectric permittivity of water increases dramatically

© 2019 John Wiley & Sons, Ltd.

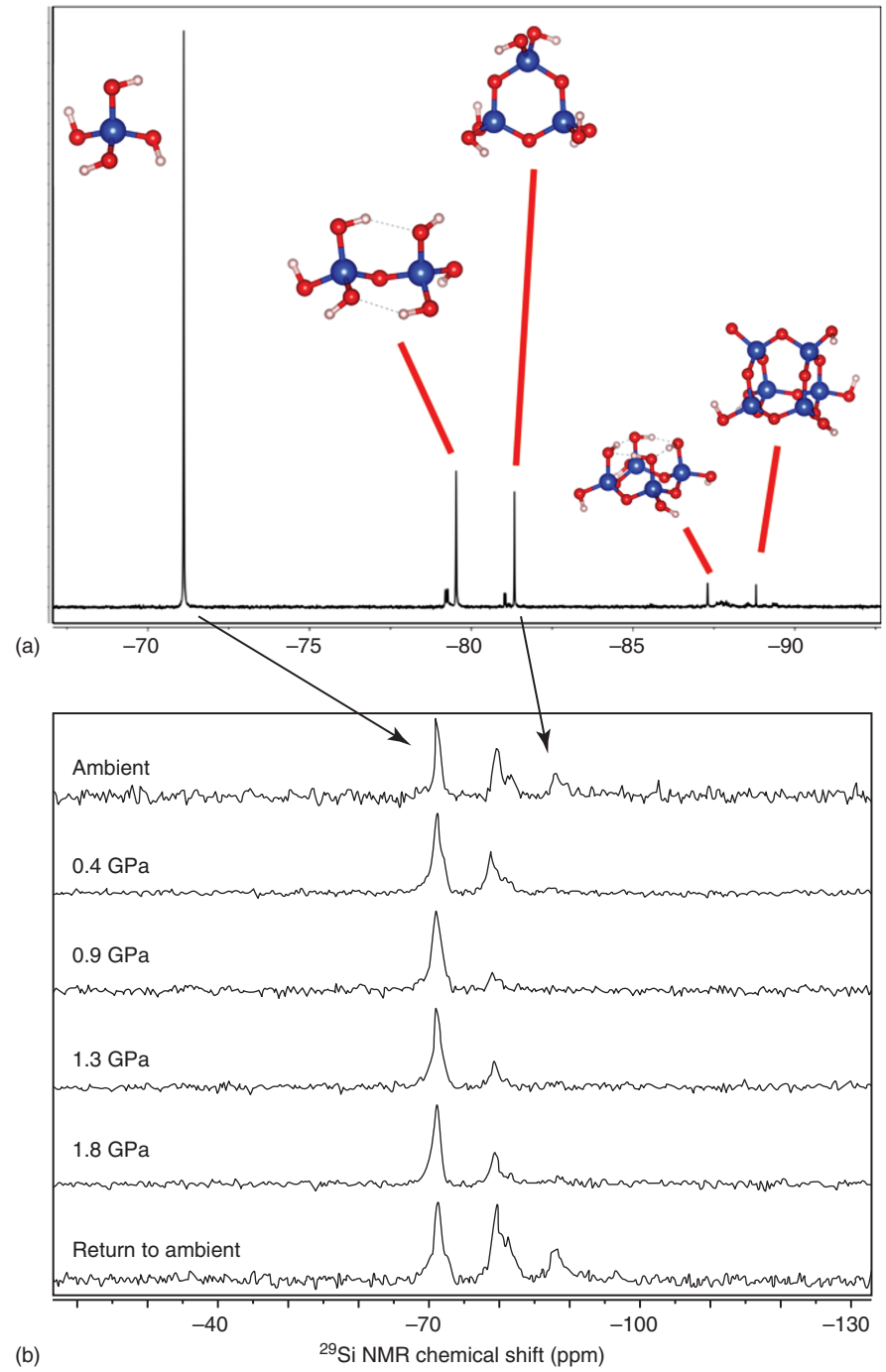

Figure 6. ^{29}Si NMR of the oligomeric silicate solution. (a) The initial solution was measured on a standard high-resolution Bruker probe, showing a series of different oligomers, with the main peak at −72 ppm the silicate monomer. (b) The high-pressure measurements on the same solution, showing a decrease in the cyclic trimer (Q^2_3) and dimer (Q^1_2) species as pressure is increased. The peaks between −85 and −90 ppm do not appear in the spectra from the high-pressure probe as the signals are below the signal-to-noise threshold.[52] (Source: Pilgrim [52], https://www.nature.com/articles/s42004-018-0066-3. Licensed under CC BY 4.0)

with pressure, to values greater than 100 at ambient temperatures and pressure less than 1.0 GPa, but drastically decreases with temperature.[67,68] This change in the dielectric of water dramatically affects the ability of water to solvate and dissociate electrolyte constituents. Thus, these probe designs open up new areas for experimental research on the properties of aqueous solutions. Clearly, adding high-temperature capabilities to the high pressure is essential to geochemists attempting to validate their thermodynamic models. Experiments are currently ongoing in this regard.

© 2019 John Wiley & Sons, Ltd.

Acknowledgments

The authors would like to acknowledge the United States Department of Energy, Office of Basic Energy Sciences, Chemical Sciences, Geosciences and Biosciences Division via Grant DE-FG0205ER15693 for their continued support in our efforts. Peter Klavins and Brian Devine are thanked for their expertise in design and construction of our designs.

Biographical Sketches

Corey D. Pilgrim b. 1985. B.Sc. University of Washington (Chemistry), 2007; Ph.D. University of California at Davis (Analytical Chemistry), 2018. CDP is just starting as a Glenn T. Seaborg Distinguished Postdoctoral Associate at the Idaho National Lab. His research has so far focused on the use of variable-temperature and variable-pressure techniques to study the kinetics of exchange and the speciation of inorganic species in aqueous solutions.

William H. Casey b. 1955, B.A. University of the Pacific (Geology), 1976; M.S. University of California Davis (Geology), 1980; PhD The Pennsylvania State University (Geochemistry and Mineralogy), 1986. His research is in aqueous solution chemistry, including aqueous interface chemistry.

Jeffrey H. Walton b. 1958, B.S. University of Florida (Physics), 1980; M.S. University of Florida (Physics), 1983; Ph.D., College of William and Mary (Physics) 1989, JHW is currently the Technical Director of the UC Davis NMR Facility. His research broadly encompasses magnetic resonance spectroscopy and imaging of materials.

Related Articles

Jonas, Jiri: NMR and High Pressure; High-Pressure NMR; Kinetics at High Pressure; High-Pressure NMR: Techniques

References

1. G. B. Benedek and E. M. Purcell, *J. Chem. Phys.*, 1954, **22**, 2003.
2. T. Kushida and L. Rimai, *Phys. Rev.*, 1966, **143**, 157.
3. G. A. Matzkanin and T. A. Scott, *Phys. Rev.*, 1966, **151**, 360.
4. R. A. Hultsch and R. G. Barnes, *Phys. Rev.*, 1962, **125**, 1832.
5. J. G. Powles and M. C. Gough, *Mol. Phys.*, 1969, **16**, 349.
6. T. A. Scott, *Phys. Rep.*, 1976, **27**, 89 (see Figure 2 and references there).
7. J. H. Walton and T. Gullion, *J. Phys. Chem.*, 1994, **98**, 13064.
8. J. H. Walton, M. J. Lizak, M. S. Conradi, T. Gullion, and J. Schaefer, *Macromolecules*, 1990, **23**, 416.
9. B. G. Pautler, C. A. Colla, R. L. Johnson, P. Klavins, S. J. Harley, C. A. Ohlin, D. A. Sverjensky, J. H. Walton, and W. H. Casey, *Angew. Chem. Int. Ed.*, 2014, **53**, 9788.
10. R. W. Peterson and A. J. Wand, *Rev. Sci. Instrum.*, 2005, **76**, 094101.
11. H. Eyring, *J. Chem. Phys.*, 1935, **1934**, 107.
12. M. G. Evans and M. Polanyi, *Trans. Faraday Soc.*, 1935, **31**, 875.
13. T. Asano and W. J. Le Noble, *Chem. Rev.*, 1978, **78**, 407.
14. R. Van Eldik, T. Asano, and W. J. LE Noble, *Chem. Rev.*, 1989, **89**, 549.
15. A. Drljaca, C. D. Hubbard, R. Van Eldik, T. Asano, M. V. Basilevsky, and W. J. Le Noble, *Chem. Rev.*, 1998, **98**, 2167.
16. H. M. McConnell, *J. Chem. Phys.*, 1958, **28**, 430.
17. T. J. Swift and R. E. Connick, *J. Chem. Phys.*, 1962, **37**, 307.
18. C. L. Perrin and T. J. Dwyer, *Chem. Rev.*, 1990, **6**, 935.
19. A. D. Bain, *Prog. Nucl. Magn. Reson. Spectrosc.*, 2003, **43**, 63.
20. L. Helm and A. E. Merbach, *Chem. Rev.*, 2005, **105**, 1923.
21. P. W. Bridgman, in 'The Physics of High Pressure', eds E. N.d. C. Andrade, G. Bell and Sons, Ltd: London, 1949.
22. E. Lisell, Om Tryckets Inflytande På Det Elektriska Ledningsmotståndet Hos Metaller Samt En Ny Metod Att Mäta Höga Tryck, Akademisk Afhandlung, E. Berling: Upsala, 1902.
23. P. W. Bridgman, *Proc. Am. Acad. Arts Sci.*, 1911, **47**, 321.
24. L. H. Adams, R. W. Goranson, and R. E. Gibson, *Rev. Sci. Instrum.*, 1937, **8**, 230.
25. R. A. Forman, G. J. Piermarini, J. D. Barnett, and S. Block, *Science*, 1972, **176**, 284.
26. G. J. Piermarini, S. Block, J. D. Barnett, and R. A. Forman, *J. Appl. Phys.*, 1975, **46**, 2774.
27. H. K. Mao, J. Xu, and P. M. Bell, *J. Geophys. Res.*, 1986, **91**, 4673.
28. D. W. McCall, D. C. Douglass, and E. W. Anderson, *Phys. Fluids*, 1959, **2**, 87.
29. A. W. Nolle and P. P. Mahendroo, *J. Chem. Phys.*, 1960, **33**, 863.
30. A. A. Brooks, E. O. Stejskal, and V. W. Weiss, *Rev. Sci. Instrum.*, 1968, **39**, 917.
31. D. E. Woessner and B. S. Snowden, *J. Chem. Phys.*, 1970, **52**, 1621.
32. J. Jonas, T. E. Bull, and C. A. Eckert, *Rev. Sci. Instrum.*, 1970, **41**, 1240.
33. J. Jonas, *Rev. Sci. Instrum.*, 1972, **43**, 643.
34. J. Jonas, T. DeFries, and D. J. Wilbur, *J. Chem. Phys.*, 1976, **65**, 582.
35. L. Ballard, C. Reiner, and J. Jonas, *J. Magn. Reson. Ser. A*, 1996, **123**, 81.
36. R. L. Johnson, S. J. Harley, C. A. Ohlin, A. F. Panasci, and W. H. Casey, *ChemPhysChem*, 2011, **12**, 2903.
37. C. D. Pilgrim, M. Zavarin, and W. H. Casey, *Inorg. Chem.*, 2017, **56**, 661.
38. L. Ballard, A. M. Yu, C. Reiner, and J. Jonas, *J. Magn. Reson.*, 1998, **133**, 190.
39. R. W. Vaughan, C. F. Lai, and D. D. Elleman, *Rev. Sci. Instrum.*, 1971, **42**, 626.
40. S. H. Lee, K. Luszczynski, R. E. Norberg, and M. S. Conradi, *Rev. Sci. Instrum.*, 1987, **58**, 415.
41. S. H. Lee, M. S. Conradi, and R. E. Norberg, *Rev. Sci. Instrum.*, 1992, **63**, 3674.
42. J. D. Barnett, S. Block, and G. J. Piermarini, *Rev. Sci. Instrum.*, 1973, **44**, 1.
43. R. Bertani, M. Mali, J. Roos, and D. Brinkmann, *Rev. Sci. Instrum.*, 1992, **63**, 3303.
44. M. G. Pravica and I. F. Silvera, *Rev. Sci. Instrum.*, 1998, **69**, 479.
45. J. Haase, S. K. Goh, T. Meissner, P. L. Alireza, and D. Rybicki, *Rev. Sci. Instrum.*, 2009, **80**.
46. T. Meier and J. Haase, *J. Vis. Exp.*, 2014, 1.
47. T. Meier, N. Wang, D. Mager, J. G. Korvink, S. Petigirard, and L. Dubrovinsky, *Sci. Adv.*, 2017, **3**, 1.
48. H. Fujiwara, H. Kadomatsu, and K. Tohma, *Rev. Sci. Instrum.*, 1980, **51**, 1345.
49. M. I. Eremets, V. V. Struzhkin, and A. N. Utjuzh, *Phys. B Phys. Condens. Matter*, 1995, **211**, 369.
50. I. R. Walker, *Rev. Sci. Instrum.*, 1999, **70**, 3402.
51. G. Ochoa, C. D. Pilgrim, M. N. Martin, C. A. Colla, P. Klavins, M. P. Augustine, and W. H. Casey, *Angew. Chem. Int. Ed.*, 2015, **54**, 15444.
52. C. D. Pilgrim, C. A. Colla, G. Ochoa, J. H. Walton, and W. H. Casey, *Commun. Chem.*, 2018, **1**, 67.
53. H. Yamada, *Rev. Sci. Instrum.*, 1974, **45**, 640.
54. A. J. Wand, E. Amherst, M. R. Ehrhardt, J. L. Urbauer, Apparatus and Method for High Pressure NMR Spectroscopy. U.S. Pat. No. 5,977,772 (Nov. 2, 1999).
55. J. L. Urbauer, M. R. Ehrhardt, R. J. Bieber, P. F. Flynn, and A. J. Wand, *J. Am. Chem. Soc.*, 1996, **118**, 11329.
56. A. J. Wand, M. R. Ehrhardt, and P. F. Flynn, *Proc. Natl. Acad. Sci.*, 1998, **95**, 15299.

© 2019 John Wiley & Sons, Ltd.

57. E. J. Fuentes and A. J. Wand, *Biochemistry*, 1998, **37**, 9877.
58. K. K. Frederick, M. S. Marlow, K. G. Valentine, and A. J. Wand, *Nature*, 2007, **448**, 325.
59. J. M. Kielec, K. G. Valentine, and A. J. Wand, *Biochim. Biophys. Acta Biomembr.*, 2010, **1798**, 150.
60. Y. A. Kozlovsky, *Sci. Am.*, 1984, **251**, 98.
61. H. C. Helgeson and D. H. Kirkham, *Am. J. Sci.*, 1974, **274**, 1089.
62. H. C. Helgeson and D. H. Kirkham, *Am. J. Sci.*, 1974, **274**, 1199.
63. H. C. Helgeson and D. H. Kirkham, *Am. J. Sci.*, 1976, **276**, 97.
64. H. C. Helgeson, D. H. Kirkham, and G. C. Flowers, *Am. J. Sci.*, 1981, **281**, 1249.
65. D. Pan, L. Spanu, B. Harrison, D. A. Sverjensky, and G. Galli, *Proc. Natl. Acad. Sci.*, 2013, **110**, 6646.
66. D. A. Sverjensky, B. Harrison, and D. Azzolini, *Geochim. Cosmochim. Acta*, 2014, **129**, 125.
67. K. Heger, M. Uematsu, and E. U. Franck, *Berichte der Bunsengesellschaft für Phys. Chem.*, 1980, **84**, 758.
68. K. S. Pitzer, *Proc. Natl. Acad. Sci. U. S. A.*, 1983, **80**, 4575.

© 2019 John Wiley & Sons, Ltd.